Scientific Research Publishing

International Journal of Geosciences, 2023, 14, 855-876
https://www.scirp.org/journal/ijg
ISSN Online: 2156-8367
ISSN Print: 2156-8359

A Case Study of Ocean-Atmosphere Interactions during the Passage of an Extra-Tropical Cyclone in the Vicinity of Cape Hatteras, North Carolina

Neil Jacobs[1*], James Churchill[2], Leonard Pietrafesa[3,4], Shaowu Bao[3], Paul Gayes[3]

[1]University Corporation for Atmospheric Research, Boulder, USA
[2]Department of Physical Oceanographym Woods Hole Oceanographic Institution, Woods Hole, USA
[3]School of Coastal & Marine Systems Science, Burroughs & Chapin Center for Marine & Wetland Studies, Coastal Carolina University, Conway, USA
[4]Department of Marine, Earth, Atmospheric Sciences, North Carolina State University, Raleigh, USA
Email: *njacobs@ucar.edu, jchurchill@whoi.edu, ljpietra@ncsu.edu, sbao@coastal.edu, ptgayes@coastal.edu, ljpietra@ncsu.edu

How to cite this paper: Jacobs, N., Churchill, J., Pietrafesa, L., Bao, S. and Gayes, P. (2023) A Case Study of Ocean-Atmosphere Interactions during the Passage of an Extra-Tropical Cyclone in the Vicinity of Cape Hatteras, North Carolina. *International Journal of Geosciences*, **14**, 855-876.
https://doi.org/10.4236/ijg.2023.149046

Received: June 12, 2023
Accepted: September 23, 2023
Published: September 26, 2023

Abstract

The authors document the interaction of the atmosphere and ocean during the formation and passage of an Extra-Tropical Cyclone, which is a Nor-Easter, winter storm that formed in the southern apex of the Middle Atlantic Bight near Cape Hatteras North Carolina, between February 15 and 18, 1996. While Nor-Easters per se, which have formed along the Atlantic Eastern Seaboard of the United States have been studied for decades, the actual atmospheric-oceanic mechanics and thermodynamics in the formation of a Nor-Easter has never been documented. We report on having done so with in-situ observations and data-based calculations and a numerical model. The in-situ observations were made via a Control Volume consisting of an array of Eulerian Oceanic-Atmospheric Moorings with current meters, temperature and salinity sensors and meteorological towers. We find that Gulf Stream waters were located surrounding the mooring array, and that with the invasion of cold dry atmospheric air, there was a rapid loss of heat from the ocean to the atmosphere via latent and sensible surface heat flux during the cyclogenesis onset of the storm. A unique feature of this storm was that neither satellite nor buoy data showed significant sea surface cooling in the control volume. The findings indicate that storm winds drove warm saline waters from the Gulf Stream across the continental shelf into the control volume, accounting for a 51 cm rise in water level along the coast. This lateral heat advection provided heat to the control volume of 3.4e+18 Joules. On average, the heat loss at the surface of the control volume, via sensible and latent heat fluxes and radiation, was 0.7e+18 Joules, corresponding to a surface heat flux of −600 Watts per Meter2 (W/m^2). However, the heat lost by the control volume as

latent and sensible heat fluxes was less than the heat it received via lateral heat advection, resulting in the lack of an often-observed sea surface cooling during other winter storms. The serendipitous and detailed observations and calculations reveal a climatological flywheel in this region, documenting the role of ETCs in the global heat balance.

Keywords

Mid-Latitude Cyclone, Extra-Tropical Cyclone, Cyclogenesis, Nor'easter Winter Storms, Latent and Sensible Heat Fluxes, Salt Flux

1. Introduction

During the fall, winter, and spring periods in the Northern Hemisphere, Atlantic low pressure systems also known variously as Nor'easters, Atlantic Lows, Cape Hatteras Lows and Extra-Tropical Cyclones (ETCs) are present over the coastal zone principally from Georgia (GA) to New Jersey (NJ) [1], extending from 25˚ to 75˚ North latitude. ETCs intensify, and often form, throughout this zone, centered about Cape Hatteras. These storms feature gale force winds, heavy precipitation, ice, coastal storm surge, intense beach erosion, and are often responsible for loss of life and severe damage along the U.S. eastern seaboard. The ETCs can deepen, *i.e.* further intensify, or spawn through a process known as "cyclogenesis" [2] and develop rapidly along and off the coast. The SC to VA coastal region is unique in its position adjacent to the warm waters of the Gulf Stream. Its alignment is favorable to the generation of offshore flow in response to winds typically associated with the incursion of cold, dry air from the north and west, often referred to as cold-air outbreaks (CAOs). The important role that ETCs play in the planetary climate system has been discussed in [3]. In that study, ETCs are shown to have a primary role in determining the local weather and its typical variation, with a strong influence on precipitation, cloudiness, radiation, and their spatiotemporal variability, and they also have an important role in the atmospheric general circulation by exercising a strong influence on the vertical and horizontal exchange of heat, moisture, and momentum, interacting with the large-scale atmospheric centers of action.

The name Nor'easter is so called because the winds over the coastal area are typically from the northeast. These storms may occur at any time of year but are most frequent and most violent between September and April. Some well-known Nor'easters include the notorious Blizzard of 1888, the "Ash Wednesday" storm of March 1962, the New England Blizzard of February 1978, the March 1993 "Superstorm" and the recent Boston snowstorms of January and February 2015. Past Nor'easters have been responsible for billions of dollars in damage, severe economic, transportation and human disruption, and in some cases, disastrous coastal flooding. Damage from the worst storms can exceed a billion dollars. Nor'easters usually develop in the latitudes between Georgia and New Jersey,

within 100 miles east or west of the East Coast. These storms progress generally northeastward and typically attain maximum intensity near New England and the Maritime Provinces of Canada. They nearly always bring precipitation in the form of heavy rain or snow, as well as winds of gale force, rough seas, and, occasionally, coastal flooding to the affected regions. The heavily populated region between Washington D.C., Philadelphia, New York and Boston, the "I-95 Corridor", is especially impacted by Nor'easters. The U.S. East Coast from Georgia to New Jersey [1], provides an ideal breeding ground for Nor'easters. During winter, the polar jet stream transports cold Arctic air southward across the plains of Canada and the United States, then eastward toward the Atlantic Ocean where warm air from the Gulf of Mexico and the Atlantic tries to move northward. The warm waters of the Gulf Stream help keep the coastal waters relatively mild during the winter, which in turn helps warm the cold winter air over the water. This difference in temperature between the warm air over the water and cold Arctic air over the land is the fuel that feeds Nor'easters.

In an extensive body of literature, it has been shown that ETC deepening and genesis processes are enhanced by the exchange of buoyancy between the ocean and atmosphere in the marine atmospheric boundary layer (MABL) ([2]-[11]) and extensive research has also been done on pre-storm air-sea interactions that lead to the spawning of these storms. These prior studies have shown that there are several factors that are involved in the development of an ETC. In particular, an excellent summary of those conditions was presented in [1], including vorticity advection, the vertical component of the curl of the frictional force becoming more cyclonic with distance from the air-sea interface, local maxima in temperature advection and diabathic heating. Statistically significant evidence of ocean influences on ETC deepening and genesis in the SC to VA region was also provided in [1]. However, none of the above studies actually documented the oceanic and atmospheric processes which occur during the genesis of an ETC via in-situ Eulerian mooring observations, particularly in the centroid of NAOB ETC genesis, near Cape Hatteras. This study reports on such a study.

The oceanographic setting in the region between SC to VA is such that the Gulf Stream Front (GSF) is omni-present near the shelf-break between 32.5˚ and 35.5˚N. The Gulf Stream is defined by a sea surface temperature (SST) of 25˚C - 28˚C, and through fall, winter and spring, it warms the overlying atmosphere [12]. However, coastal waters in this same domain have surface temperatures typically in the range of 6˚C to 9˚C during the winter months, and up to 20˚C in the late spring and early fall [12]. The land surface generally has temperatures varying from 0˚C to 10˚C, in the mid-winter, depending on the time of day [13] with air temperatures ranging from 0˚C to 25˚C. During occasions of incursions of cold dry air streaming into the area from the north, local air temperatures can drop to between 0˚C to 10˚C, hence a CAO. The net effect is a large across-shelf air temperature differential which produces a highly baroclinic structure throughout the MABL. In [1] it was determined that the strength of the MABL baroclinicity is dependent on the ratio of the offshore-onshore air temperature

difference to the distance of GSF from the coast. Further, their study showed that intensification of coastal cyclones was strongly correlated to pre-storm baroclinicity. Finally, and very significantly, results from the study in [1] which reveal that the rate of surface cyclonic intensification was linked to both the thermal structure of the continental air mass and the position of the GSF, in relation to land. However, the distance of the GSF from the coast can fluctuate significantly.

Lateral meandering of the GSF makes the distance from the position of the GSF vary significantly [14]. The meander phenomenon is, in part, a manifestation of the down stream propagation of Topographic Rossby Waves (TRWs) created at the site of a topographic bottom feature offshore Charleston, SC located at 32˚N and 79˚W also known as the Charleston "bump" ([12] [15]). Two studies ([12] [16]) revealed 2 - 12 day lateral dynamics of the GSF from the Straits of Florida to Cape Hatteras NC. The lateral meanders of the GSF and the TRWs were found to travel with wavelengths the order of 80 - 300 km, and lateral amplitudes up to 20 kilometers (km) [14]. As the TRWs pass, the wave crest or onshore manifestation of the wave may be located close to the coast for a 1 - 7 day period. Thus, the location of the GSF will affect the measure of baroclinicity of the MABL in the region. Still there are other factors important in ETC deepening or formation.

As discussed in [1] and [17], the effects of differential geostrophic vorticity advection on the deepening or formation of an ETC arise from atmospheric wave-trains at the 500 mb level. In a series of baroclinic ridges and troughs, vorticity maxima (minima) are located along the trough (ridge) axes. Downstream from a maxima in absolute vorticity is a zone of cyclonic vorticity advection. Since there is rising motion downstream from the trough, cyclonic vorticity increases with height. In the region of cyclonic vorticity advection, the effect of differential vorticity advection is to make the atmospheric surface pressure fall. This falling pressure contributes to the formation of surface troughs, or atmospheric cyclones. Temperature advection along a frontal zone can aid in the formation of a surface cyclone provided there is a pre-existing trough. Rising motion can be found in the warm frontal zone extending from the central low pressure at the 500 mb level. This rising motion, caused by the warm advection, can also abet the formation of a trough at the surface. Quasigeostrophic effects of surface friction above gradient-wind level are negligible; hence the vertical component of the curl of the friction force is zero. However, in the friction layer, if the vertical component of the curl of the friction force is anticyclonic, then the vorticity is cyclonic. At the gradient-wind level, the vertical component of the curl of the friction force becomes less anticyclonic with height. Therefore, there is rising motion which can result in a trough formation at the surface level. The final effect responsible for the formation of a surface cyclone is bottom boundary layer heating. This occurs when cooler, drier continental air moves over warmer water. The flux of sensible and latent heat into the atmosphere also can aid in the formation of a surface low. However, fluxes of heat from ocean to atmosphere

during event passage or genesis have not been well documented. Serendipity in oceanic-atmospheric observations is required to observe ETC genesis and/or passage.

Explosive development of an ETC can also be influenced by strong wind velocities. CAOs occur when strong northerly quadrant winds force cold air further south. About 15 to 20 of these events occur annually from September through April, and last for 1 to 3 days ([3] [17] [18]). The winds most favorable for preconditioning to occur off the coast of the Carolinas, are from a north to northwesterly direction. These winds typically result from the presence of a strong anti-cyclone over the continent. This high usually moves southeast out of Canada into the northeastern continental U.S. sending a dome of cold air with its strong northerly to northeasterly winds. This phenomenon is known as cold-air damming [17] [19]. The high-pressure system holds the warm front far to the south while a low-pressure system is often present or can sometimes form off the coast due to the increased thermal gradient. Extensive research has gone into studying these events and how they relate to the MABL ([20]-[29]). Nonetheless, and to reiterate, the actual coupled process of air-sea interaction during the passage of an ETC has not been documented in the literature.

During the period February-May, 1996, a U.S. Department of Energy (DOE) sponsored an oceanographic and meteorological physical and bio-geochemical observational program called the Ocean Margins Program. This was staged in the continental margin region between Cape Hatteras, NC and Chesapeake Bay, VA., and included data collection from 39 moorings at 27 locations [30]. In addition to the data from this program, other marine and atmospheric data were obtained from National Oceanic & Atmospheric Administration (NOAA) monitoring programs. These data included marine meteorology measurements, coastal sea levels and NOAA GOES AVHRR satellite data. Using these data and models, we will study an ETC that was present over and across the OMP array over the period February 15-19, 1996.

2. Materials and Methods

The OMP moored instrument array described in [30] was designed to measure a comprehensive suite of biological, chemical, sedimentological, meteorological, and physical oceanographic processes over the shelf and slope between the Chesapeake Bay, VA, and Cape Hatteras, NC. The cross-isobath and along-isobath array of instruments included a high resolution control volume (<15 km with a 10 km half diagonal) on the northern end of the mooring array in 40 m of water (**Figure 1(a)**). This design was intended to measure processes, both horizontally and vertically, operating over a wide wide range of scales (roughly 10 - 150 km). The array's northern and southern across-isobath lines (NL and SL, respectively), provided measurements of input and output to the study region, *i.e.* along-isobath flow through cross-isobath lines. An along-isobath picket fence of moorings was located along the 75 m isobath to capture cross-isobath sources and

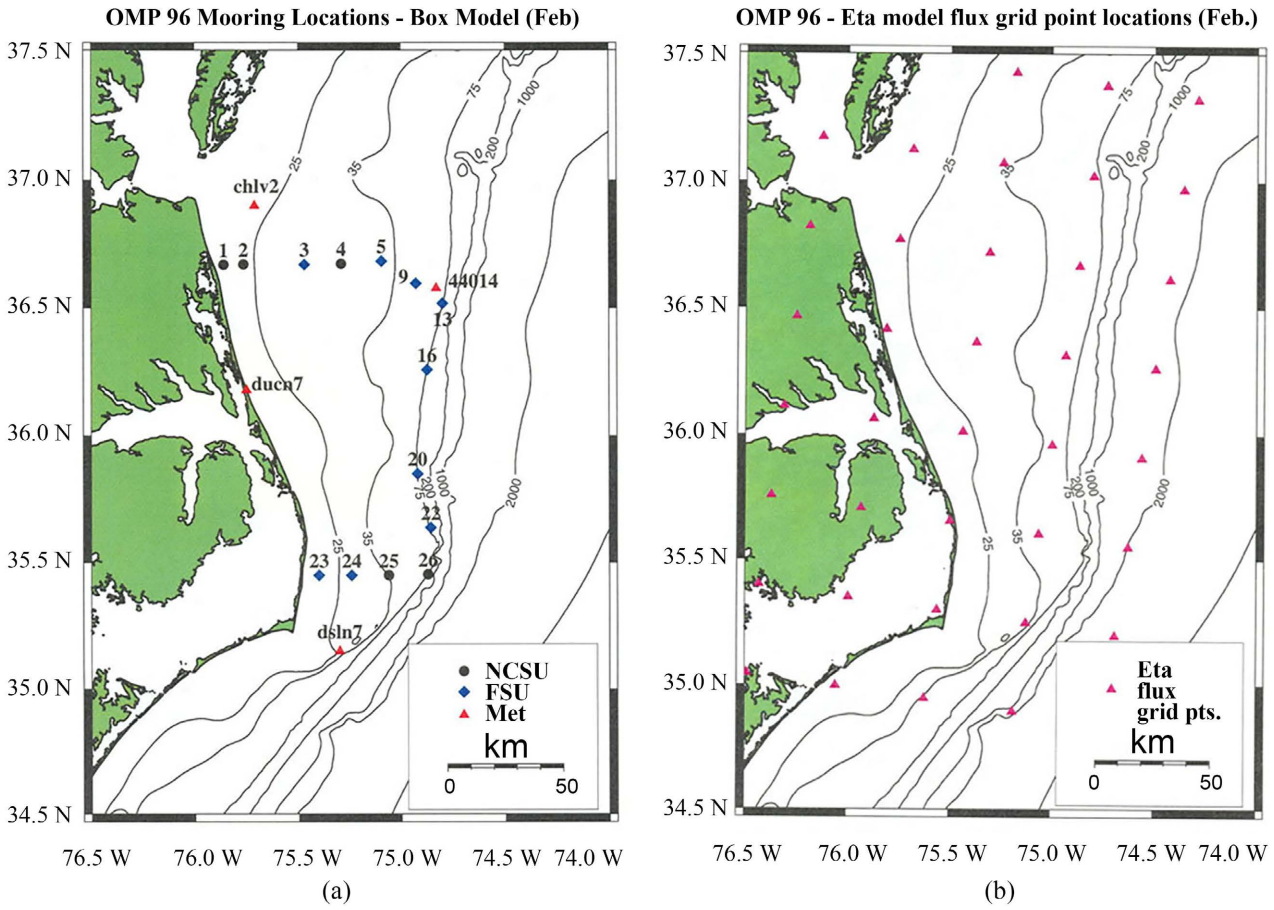

Figure 1. (a) Left panel, ocean margins program DOE mooring, and NOAA NDBC buoy and CMAN and NOS coastal sea level locations used in control volume calculations. Refer to [1] for instrument information and site locations; (b) right panel, NOAA Eta numerical model calculation grid point locations.

sinks from or to the slope region. The NL consisted of eight moorings (#s 1 - 8) in waters ranging in depth from 13 m to 850 m. The SL line consisted of six moorings (#s 23 - 27) in waters ranging from 20 m to 830 m depth. There were seven moorings (#s 7, 13, 16, 17, 20, 22, 26) located along the 75 m isobath. The array was deployed 1-16 February, recovered 08-16 May 1996, and then redeployed for a second period from June-October 1996. We will consider the data from the late winter to early spring measurement period. In **Figure 1(b)**, the Eta numerical model (described below) computational points are also shown for comparison to the observational array (**Figure 1(a)**).

Standard meteorological data from stations within the OMP study area are available from the National Data Buoy Center (NDBC) archives. The data set includes wind speed, wind direction, peak gust speed, significant wave height, average wave period, dominant wave period, mean wave direction, station visibility, air temperature, sea surface temperature, and coastal sea level. The NOAA National Center for Environmental Prediction (NCEP) Eta operational forecast model was used to analyze atmospheric forcing ([31] [32] [33] [34]). This model produced surface radiative, sensible, and latent heat flux values (in W/m^2) over a

spatial grid and averaged over three hour periods. The model grid is presented in **Figure 1(b)**. Validation of the model was done through additional calculations of sensible heat flux using the meteorological data sets from NDBC stations. In addition, NOAA Advanced Very High Resolution Radiometer (AVHRR) data, collected and processed by NCSU from NOAA GOES Polar Orbiting satellites, were utilized in the study. These data are not shown here, but the imagery is available in a technical report [34] and in [30].

A three-dimensional quasi-rectangular, virtual, control volume (CV) was created by forming sides from the array of moorings (**Figure 1(a)**). Side 1 faces north, formed from moorings 1, 2, 3, 4, and 5 connecting the adjacent NC coastline to Side 2. Side 2 faces northeast, formed from moorings 5, 9, and 13. The moorings forming Side 3 were 13, 16, 20, 22, and 26. This side faces east and runs along the 75 m isobath. Side 4 faces south and connects the NC coast to Side 3 via moorings 23, 24, 25, and 26. The CV is bounded by land on the west side and by the sea floor. The 5th side is the air-sea interface, the free surface.

The volumetric balance and flux of salt is computed using mooring data of current speed and direction, and salinity at the open sides of the CV. The heat balance is computed from moored measurements of temperature and current speed and direction acquired along the sides of the CV and from flux data collected at the surface. Heat, salt and water volume fluxes, calculated through the sides of the CV, are defined such that a positive flux is directed into the CV and a negative flux is out of the CV. The perpendicular to the CV side is 90 degrees clockwise from that side in numerical mooring order. Thus, there is a manual sign change for Sides 1, 2, and 3, because the defined negative direction is actually into the CV. Therefore, the sign of Sides 1, 2 and 3 are changed to positive. The positive direction of Side 4 is into the CV.

To form the matrix of flux grid points, spatial averaging is affected between the sensor locations on each side of the CV. This calculation is applied to the orthogonal horizontal velocity components u (positive East) and v (positive North), temperature (T), and salinity (S). Spatial averaging is carried out in the x and y coordinates via the equations:

$$\frac{\partial A}{\partial x_i} = \frac{A_{i+1} - A_{i-1}}{\Delta x_{i-1} + \Delta x_{i+1}} \tag{1}$$

$$\frac{\partial A}{\partial y_i} = \frac{A_{i+1} - A_{i-1}}{\Delta y_{i-1} + \Delta y_{i+1}} \tag{2}$$

where A represents either u, v, T or S. Fluxes are then calculated using u and v for volumetric flux; u, v, and S for salt flux; and u, v, and T for heat flux. These values are then interpolated over the surface area of the side for the net flux of that particular side.

The NOAA Eta-coordinate model ([31] [32] [33] [34]) is used to determine atmospheric forcing. The model produces data on a latitude and longitude grid (**Figure 1(b)**). The model output includes surface radiative, latent, and sensible heat fluxes in W/m^2, averaged over 3 hours.

The net heat transfer, Q_{eta}, is obtained by summing the individual 3-hour flux averages and multiplying by this time interval.

$$Q_{eta} = \int_{t_1}^{t_2} \frac{\mathrm{d}Q_{atm}}{\mathrm{d}t}\mathrm{d}t = \sum_i \left.\frac{\partial Q_{atm}}{\partial t}\right|_i \Delta t_i \tag{3}$$

where $\mathrm{d}Q_{atm}/\mathrm{d}t$ is the 3 hour flux average value at a particular grid point and Δt_i = 3 hours.

Validation of the numerical model is done through an external calculation of sensible heat flux, Q_s, using the following relation:

$$Q_s = -\frac{c_p pvC_h\left(T_a - T_w\right)}{T_a R} \tag{4}$$

where c_p is the specific heat of air at constant pressure (1000 J/kg/˚C), C_h [17], is the bulk aerodynamic coefficient for the vertical transfer of sensible heat (assumed constant and equal to 0.0013), v is the average hourly wind velocity, and T_a and T_w are the average hourly air and sea surface temperatures and R is the universal gas constant. The calculations are done using the meteorological data obtained from the NDBC stations NDBC Marine Buoy 41014, dsln7 and chlv2 (**Figure 1(a)**) and plotted against the Eta model output on the model grid (**Figure 1(b)**). An additional validation is offered via weather forecasts following several prior studies in-kind [35]. Calculations are also made for the latent heat flux.

Eta model calculated radiative fluxes are separated into short-wave upward (up), Q_{swu}, short-wave downward (down), Q_{swd}, long-wave up, $Q_{lwu\ up}$, and long-wave down, $Q_{lwd\ down}$. Once again, the signs for the fluxes were changed based on their direction through (into or out of) the CV box surface.

The total heat budget from over a period t_1 to t_2 is defined by the following equation:

$$Q\left(\Delta t\right) = Q_{adv}\left(\Delta t\right) + Q_{sfc}\left(\Delta t\right) + Q_{in}\left(\Delta t\right) \tag{5}$$

where Q_{adv} is the thermal advection, Q_{sfc} is the net surface heat exchange, and Q_{in} is the rate of evolution of heat from internal sources. However, Q_{in} is frequently ignored because of its negligible contribution to the overall heat budget (Dera, 1992). For our application of these equations, all sources and sinks of heat are accounted for along the boundaries and no internal heat sources Q_{in} are considered, yielding:

$$Q\left(\Delta t\right) = Q_{adv}\left(\Delta t\right) + Q_{sfc}\left(\Delta t\right) \tag{6}$$

The term Q_{adv} has the following integral:

$$Q_{adv}\left(\Delta t\right) = \int_{t_1}^{t_2}\int_A Q_u \mathrm{d}A\mathrm{d}t \tag{7}$$

where Q_u is integrated over the surface area of a particular side and then integrated over the time period. Q_u is the thermal advection flux flowing across this side:

$$Q_u = u_j \frac{\partial\left(\rho c_p T\right)}{\partial t x_j}\mathrm{d}x_j \tag{8}$$

For the CV, advective heating is estimated as:

$$\int_{t_1}^{t_2}\int_{A_j} Q_{u_j}\,\mathrm{d}A_j\mathrm{d}t = -\int_{t_1}^{t_2}\int_{A_1} Q_1\mathrm{d}A_1\mathrm{d}t - \int_{t_1}^{t_2}\int_{A_2} Q_2\mathrm{d}A_2\mathrm{d}t - \int_{t_1}^{t_2}\int_{A_3} Q_3\mathrm{d}A_3\mathrm{d}t + \int_{t_1}^{t_2}\int_{A_4} Q_4\mathrm{d}A_4\mathrm{d}t \quad (9)$$

The negative signs preceding the first three terms denote a positive flux in the south and west directions, whereas the positive sign preceding the fourth term denotes a positive flux in the north direction.

The term, Q_{sfc}, in Equation (6) is expressed by the following integral:

$$Q_{sfc}\left(\Delta t\right) = \int_{t_1}^{t_2}\int_{A_0}\left(Q_r - Q_b - Q_l - Q_s\right)\mathrm{d}A_0\mathrm{d}t \quad (10)$$

where Q_r is the solar radiation flux absorbed by the sea, Q_b is the effective IR flux radiated by the sea surface, Q_l is the latent heat flux, and Q_s is the sensible heat flux. Q_{sfc} is evaluated by integrating Equation (3) over the surface area of the CV, A_0, and then integrating over time

$$Q_{sfc}\left(\Delta t\right) = \int_{t_1}^{t_2}\int_{A_0}\left(\sum_i \left.\frac{\partial Q_{atm}}{\partial t}\right|_i \Delta t_i\right)\mathrm{d}A_0\mathrm{d}t \quad (11)$$

When applied to the data format provided by the Eta-coordinate model, the summation takes the following form:

$$\sum_i \left.\frac{\partial Q_{atm}}{\partial t}\right|_i \Delta t_i = \left(\frac{\partial Q_{swd}}{\partial t} - \frac{\partial Q_{swu}}{\partial t} + \frac{\partial Q_{lwd}}{\partial t} - \frac{\partial Q_{lwu}}{\partial t} - \frac{\partial Q_l}{\partial t} - \frac{\partial Q_s}{\partial t}\right)\Delta t_i \quad (12)$$

where the 3-hour averages of short-wave up, Q_{swu}, short-wave down, Q_{swd}, long-wave up, Q_{lwu}, and long-wave down, Q_{lwd}, radiation are summed according to their direction into or t out of the control volume and i = 3 hours.

Substituting Equations (9) and (11) into Equation (6), the final expression for the heat budget of the CV is:

$$Q\left(\Delta t\right) = \int_{t_1}^{t_2}\int_{A_j} Q_{u_j}\,\mathrm{d}A_j\mathrm{d}t + \int_{t_1}^{t_2}\int_{A_0}\left(\sum_i \left.\frac{\partial Q_{atm}}{\partial t}\right|_i \Delta t_i\right)\mathrm{d}A_0\mathrm{d}t \quad (13)$$

3. Results

The meteorological event that we focused on was preceded by a pre-storm conditioning period of about 24 hours beginning 00Z 15 February 1996. During this time, primary and secondary low-pressure centers moved offshore of the northeastern US, and the trailing cold front remained over the southeast US becoming stationary. Genesis of the central low pressure event along this front then began its formation, as depicted in atmospheric pressure maps created by NOAA at the time. Within a period of 6 hours, beginning at 06Z 16 February, the system began to reform into a coastal low offshore of southeast NC. The coastal low then deepened rapidly as it moved northeast along the coast. The lowest pressure at 09Z 16 February was 1000 mb, and was located southwest of Wilmington, NC. Contemporaneously, a second area of weak low pressure was also evident east of Cape Hatteras, NC. Within 3 hours, at 12Z 16 February, the lows combined just southeast of Cape Hatteras with a central low pressure of 996

mb (**Figure 2(a)**). Between 12Z and 15Z on 16 February, the center of the system, still at 996 mb, entered the mooring array (our CV) from the southwest. As the low tracked across the CV, it strengthened, dropping 5 mb in 3 hours, from 996 mb at 15Z to 991 mb at 18Z 16 February. By 21Z 16 February, the system became occluded, and the center of the low, then at 989 mb, tracked northeast out of the CV. The system reformed a second time as it moved northeast, dropping from 988 mb at 03Z to 987 mb at 06Z 17 February. The pressure gradient on the backside of the low was further enhanced by a high-pressure system of 1024 mb centered over south Alabama.

AVHRR imagery (**Figure 2(b)**) collected at the time [36] reveals, through openings in the storm clouds, relatively warm, South Atlantic Bight water to the south of Cape Hatteras at the outset of the event, followed by evidence of cool Middle Atlantic Bight waters breeching Diamond Shoals as the storm matured and moved north. Following the passage of the system, the southward flow relaxed and turned eastward in the southern portion of the CV due to the lack of mechanical surface forcing from the wind and the relaxation of the buildup of water against the north side of Diamond Shoals, in keeping with dynamically processes associated with northerly wind events as described in [30]. We now revisit the fluxes observed during the event passage. It is of note that the Muti-Channel Sea Surface (MCSST) product, produced by the National Aeronautics & Space Administration (NASA) which removes cloud-cover, is presented in **Figure 2(c)** for February 13, and displays a crowding of the SST isotherms at and to the north of Cape Hatteras. An outline of the basic concepts of cloud filtering and atmospheric attenuation corrections used in the MCSST, along with the operational procedures and products are described in detail in [37].

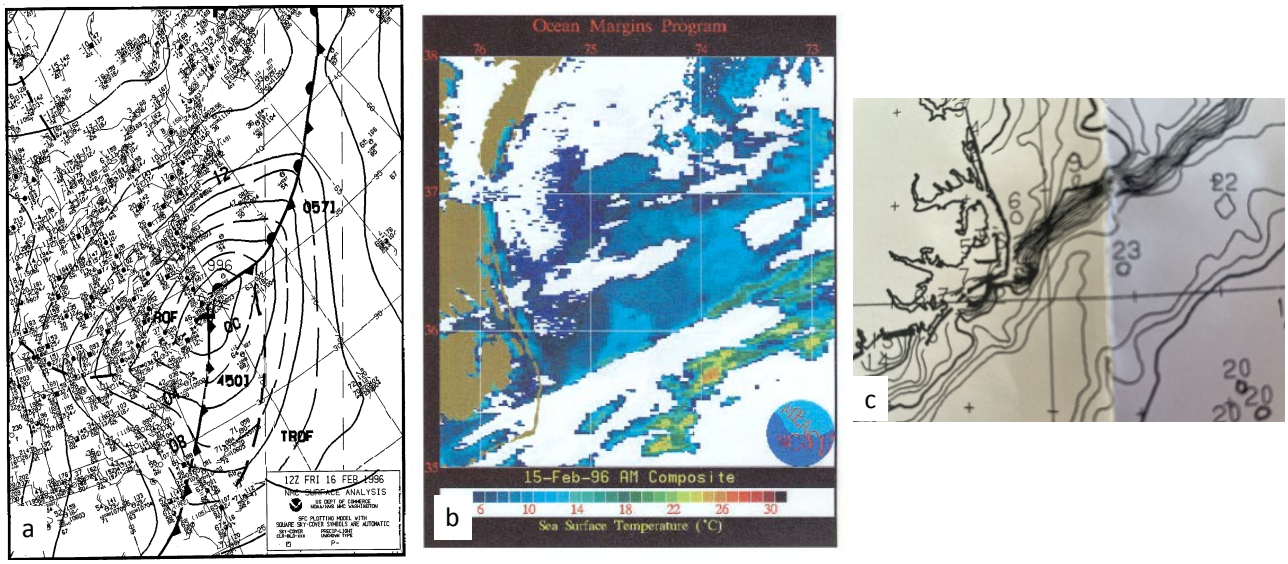

Figure 2. ETC 12, 15 February 1996. (a) Left panel NOAA NWS surface pressure field analysis at 12Z 16 showing the central low pressure field as the storm formed offshore centered east of Cape Hatteras, NC; (b) center panel s the NOAA AVHRR SST satellite mage of the ETC presence via the white cloud cover; right panel is the MCSST depiction of the SST's seaward of Cape Hatteras on February 13, displaying warm Gulf Stream waters in the OMP CV.

Moving from south to north along the boundary of the CV, the coastline is aligned north and then north-northwest and then north. In the ETC event of the February 15-19, the dominant wind was northerly to northwesterly or generally parallel to the NC coastal boundary of the CV. As shown in [30], the wind-field mechanically drove near surface shelf waters toward the south and also westward towards the coast in keeping with time dependent Ekman theory in the region ([38] [39]). As a consequence of the shoreward transport, water level rose along the coast, as manifested by the sub-inertial frequency 69 cm rise in coastal sea level shown in the data time series collected at the Duck, NC station (**Figure 3**) at the coastal boundary center of the CV (**Figure 1(a)**). Wind speeds and air minus sea surface temperatures collected at NDBC buoy 41014 and CMAN station CHLV2 (**Figure 1(a)**) are presented in **Figure 4**.

Heat advection through the sides of the CV was calculated using both 40-hour and 3-hour low pass (HLP) filtered data sets, created with use of a Lanczos-Cosine-Filter [40]. However, save for the sea level time series shown in **Figure 4**, our interest is in entire temporal suite of fluxes, so we will limit ourselves to the 3-HLP hourly sub-sampled data. Contours of these heat fluxes through each side of the control volume are shown in **Figure 5**. In these contours, sign of + (−) denotes flux into (out of) the CV, though the figures display the sign convention prior to the manual sign convention change. The heat advection values were summed to obtain the net advective heat change through each side. Over the entire event, the net amount of heat passage was: $+3.13e^{+19}$ J through Side 1 (**Figure 6(a)**), $+1.49e^{+19}$ J through Side 2 (**Figure 6(b)**), $-1.83e^{+19}$ J through Side 3

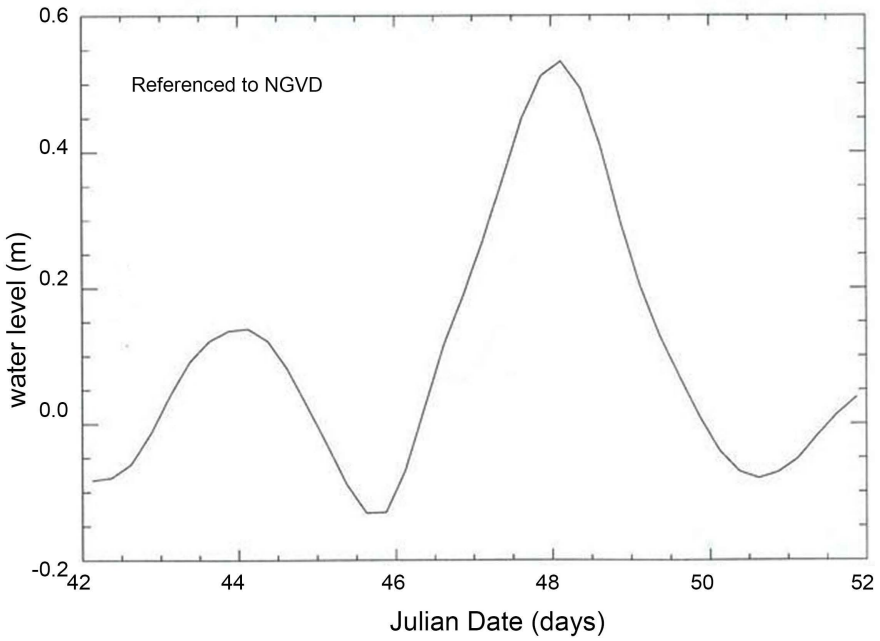

Figure 3. Water level at the NOAA NOS Duck, NC site over the period 11-21, February 1996. Raw data has been filtered as described below and then sub-sampled hourly to eliminate sub-inertial frequency motions to represent the storm induced time dependent coastal Ekman transport which resulted in a rise of 51 cm at the coast.

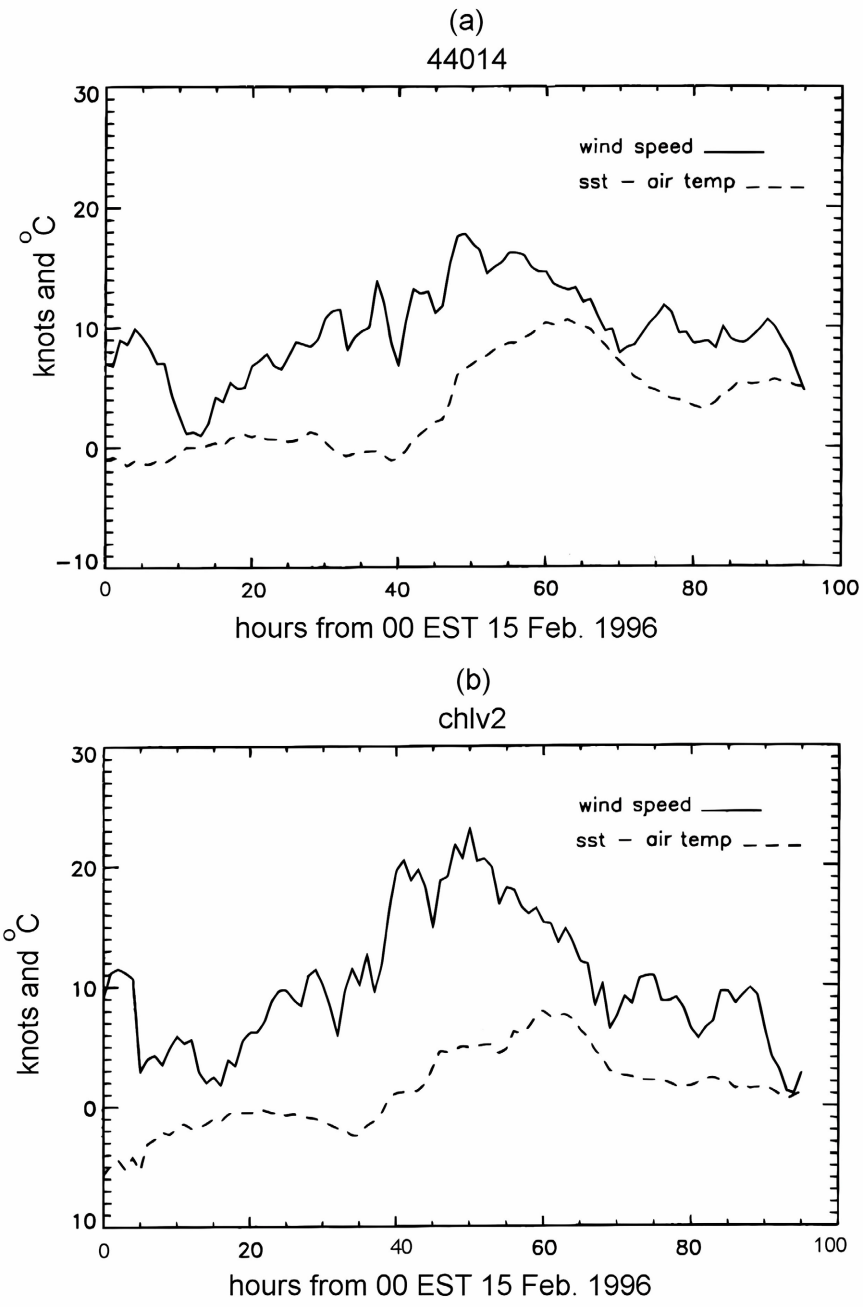

Figure 4. Wind speed and air minus sea surface temperatures over the period 15-18 February 1996 at the: (a) NOAA NDBC buoy 41014; and (b) NOAA NDBC CMAN station CHLV2. Refer to Figure 1a and [30] for site locations.

(**Figure 6(c)**) and -2.45^{+19} J through Side 4 (**Figure 6(d)**). Summing the heat gains to and losses from the CV as a result of advection yields a net gain of heat of $+0.34e^{+19}$ J.

The surface heat flux was calculated by summing the gains or losses due to sensible, latent, short wave and long wave heat fluxes through the surface of the CV. **Figure 6(a)** displays the time series of sensible heat flux over the period of the storm computed from the NDBC buoy data (dashed line) and from Eta (solid

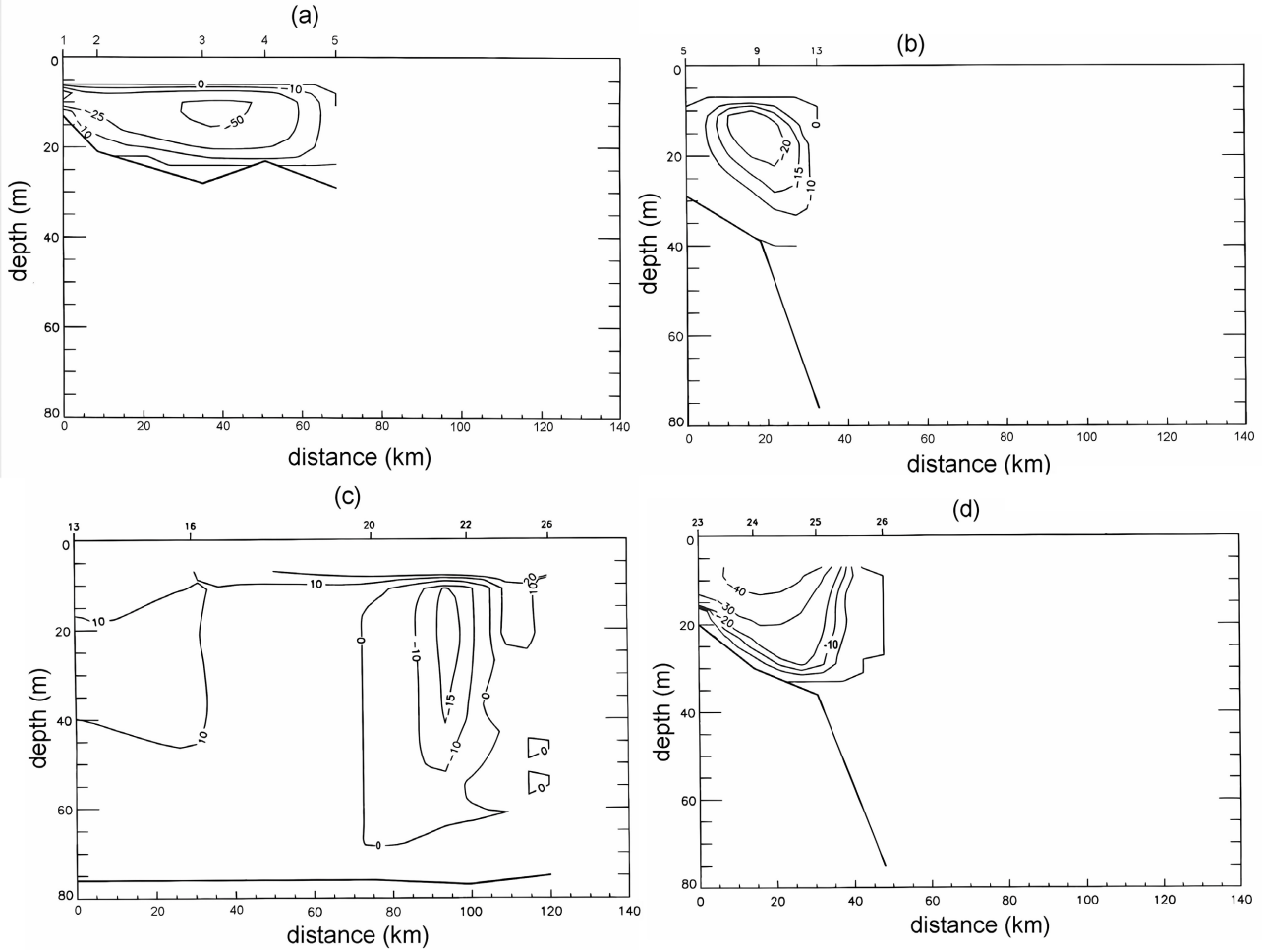

Figure 5. Cumulative heat flux contours into and out of the control volume using the 3 hour low passed mooring data over the period 15-19 February 1996: (a) through Side 1; (b) through Side 2; (c) through Side 3; and (d) through Side 4. Refer to text for details.

line) at the model domain location of the buoy. **Figure 6(b)** shows the Eta model output of latent heat flux at the site of the NDBC buoy. Over the period of the event, the Eta model gave a sensible heat transport across the CV surface of $-8.002e^{17}$ J (*i.e.*, a net heat loss) and latent heat transport through the surface of $-1.368e^{18}$ J. **Figure 7(a)**, **Figure 7(b)** show representative surface contours of sensible and latent heat fluxes, respectively, across the entire CV model surface. Note that the contours are representative of the general path of the storm. The Eta model hindcasted a shortwave radiation import to the CV of $+5.515e^{17}$ J, and a shortwave radiation export from the CV of $-9.738e^{16}$ J. Eta hindcasted the longwave radiation downward, and the longwave radiation upward to have been $+9.931e^{17}$ J and $-1.34e^{18}$ J respectively.

Summing the net gains and losses of heat across the surface CV domain gives in a net loss of heat of $-2.06e^{18}$ J. The surface area of our CV is estimated to be ~10,000 km^2 yielding an average surface heat flux of −596 W/m^2. However, to compute the total balance, the net heat lost through the surface must be subtracted from the heat gained via the net advection of heat into the CV. Thus, the

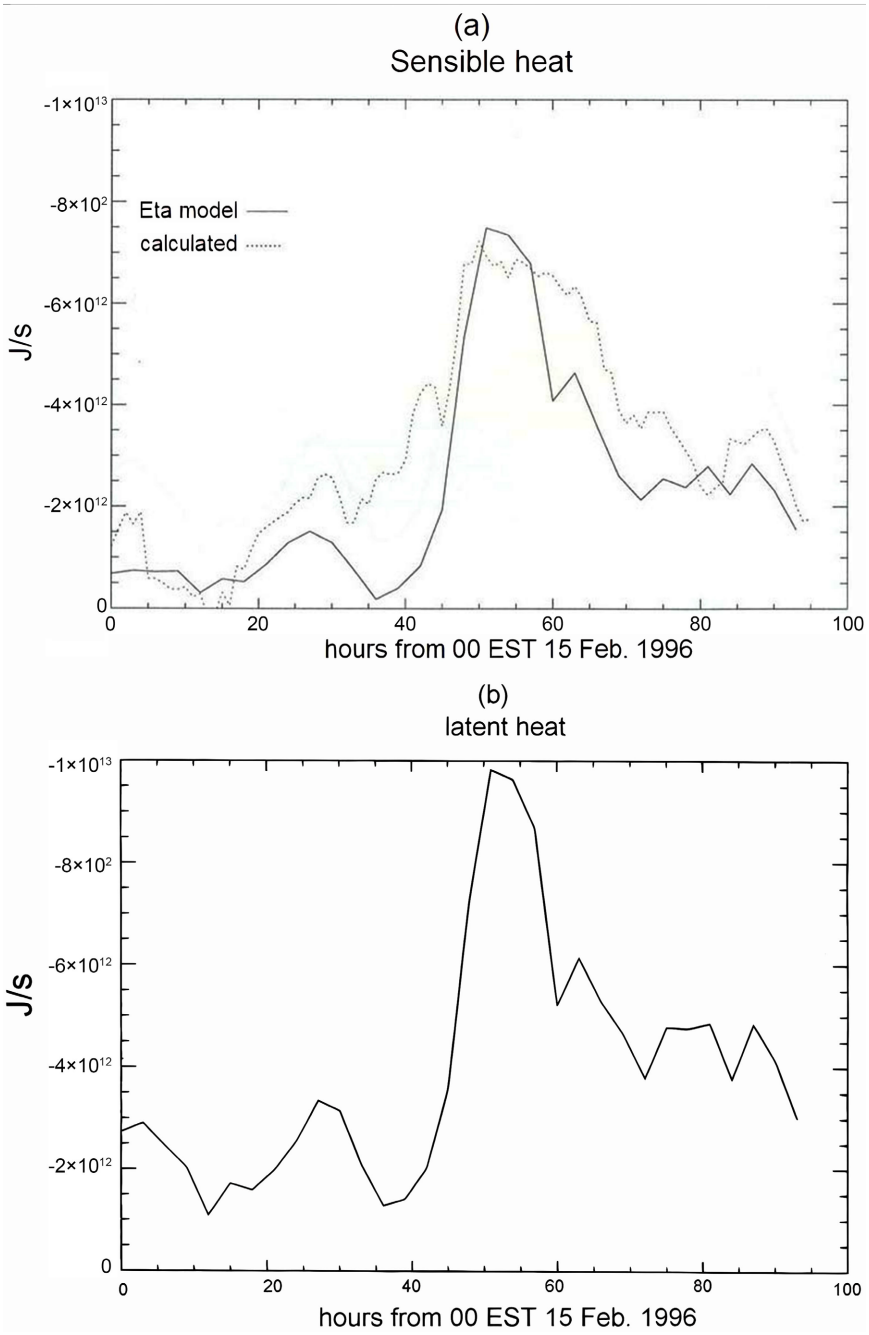

Figure 6. Sensible (observed and modeled) and Latent (modeled) heat fluxes across the surface of the Control Volume over the period 15-19 February 1996: (a) sensible heat Eta model output (solid line) and computed from observations made at the NDBC buoy and CMAN stations (dotted line); and (b) latent heat Eta model output. Long and short wave radiative flux calculations are not shown. Refer to text for details.

total net heat change in the CV results in a net increase of $+2.74e^{18}$ J. While there is a measure of uncertainty in the estimates, given the assumptions of interpolations across the CV walls, this is a very interesting result as will be discussed below.

The estimated net losses of heat through the surface of our CV and through

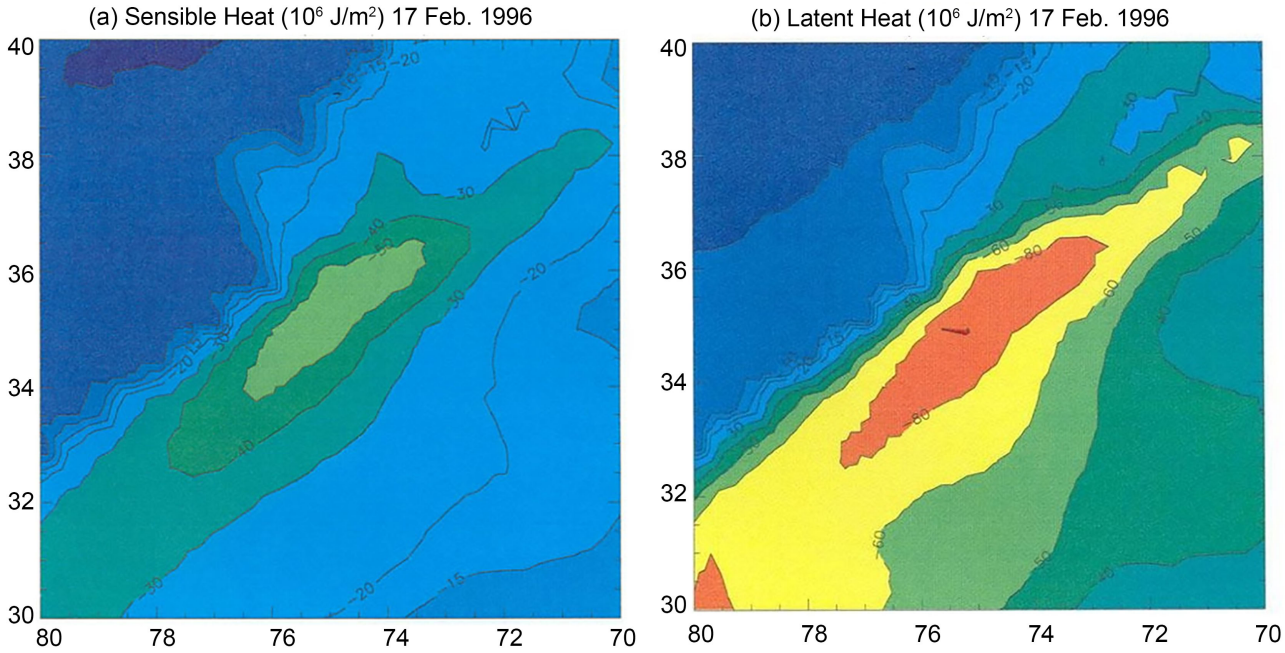

Figure 7. Representative surface heat flux swaths computed from the NOAA NWS Eta model for 17 February 1996: (a) sensible heat field; and (b) latent heat field.

the southern boundary (Side 4) are not surprising. A study of air-sea interactions during the intensification or spawning of ETCs [1] have shown that the Gulf Stream can, in the presence of a CAO, create the initial conditions for the modification of the MABL, and can effect the baroclinicity necessary to further fuel or to pop a storm. This study, and those it references, also credits Carolina coastal waters as being the source for the heat which actually fuels the storms. It is clear that the presence and location of the Gulf Stream plays a key role in affecting the strength of baroclinicity that must exist in the intensification or spawning of atmospheric coastal lows in this region. However, a serious issue has not been resolved in investigations of these storms. Basically, if there are nominally of the order of 15 - 20 of these storms within the region annually, and each extracts heat from coastal waters, then what is the source of the heat reserve? How is replenished between storms? Or, alternatively, is it not replenished?

One answer is that GSF meanders could continue to supply heat to the outer shelf; that perhaps heat could be added to shelf waters throughout the September through April period through lateral diffusion from offshore. But, lateral diffusive processes could take the order of months rather than days to resupply heat to the mid to outer shelf. Alternatively, the direct presence of GSF meanders, waves in mid shelf waters would provide the needed presence of a heat source. But, the flaw in this argument is that [14] showed that while during the late spring through summer to early fall period, GSF meanders routinely extend shoreward to the 30 m isobath on the NC shelf, during the winter months due to cooler inner shelf waters and subsequent density blocking, these events do not

penetrate shoreward of the 40 m isobath, which is in the mid-shelf. So, a mechanism other than the direct presence of GSF meanders in mid-shelf waters is necessary to fuel winter storms.

We also realized a net increase of volume and salt in our CV during the ETC passage. The fluxes of salt follow those of volume and are shown in **Figures 8(a)-(d)**. In the calculation of the volumetric flux (not shown) over the period of the storm (0000EST 15-0000EST 19 February) the volumes of water entering Sides 1 and 2 were $4.26e^{+10}$ m^3 and $2.68e^{+10}$ m^3 respectively. The volumes of water exiting Sides 3 and 4 were $1.31e^{+10}$ m^3 and $5.12e^{+10}$ m^3 respectively. Summing these values yields an increase of $0.51e^{+10}$ m^3. Since the surface area of the control volume is ~10,000 km^2, then the sea level rise associated with the storm, can be estimated as an increase in sea level of 51 cm. This sea level rise accompanying the storm is also in keeping with the results of prior studies of sea level response to wind forcing in the region [38] and agrees with the 51 cm rise above the long term mean sea level that was observed during the storm. Note that the total sea

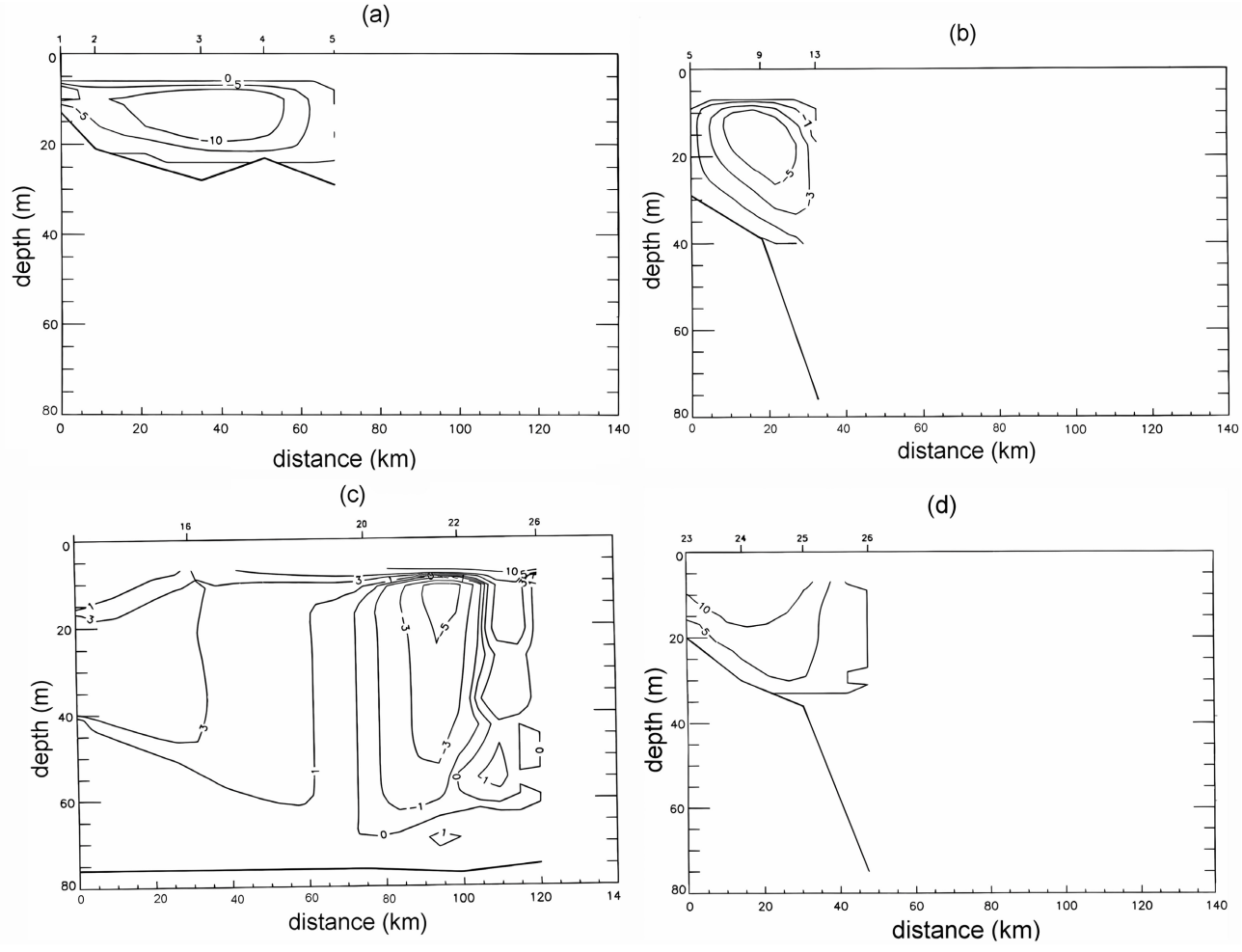

Figure 8. Cumulative salt flux contours into and out of the control volume using the 3 hour low passed mooring data over the period 15-19 February 1996: (a) through Side 1; (b) through Side 2; (c) through Side 3; and (d) through Side 4. Refer to text for details.

level during the storm was 69 cm, but 18 cm of this could either have entailed bringing the sea surface back to the equilibrium level (the long term mean) following the depression of sea level that preceded the storm event (**Figure 4**) or it might suggest that there was a drop of sea level across the shelf. The data do not allow the calculation of a proper vertical integral to determine the across shelf surface height so that estimate is not made.

The ETC event that has been documented demonstrated that there was a net gain of heat in our CV during the event passage. The conclusion is that the Gulf Stream not only conditioned the MABL but also became a source for warm waters that are mechanically driven by storm winds onto the shelf where it might become available to fuel future storms. Thus, we have identified a regional environmental flywheel. This could explain why the centroid of ETC intensification in the North Atlantic is the southern apex of the mid-Atlantic Bight ([1] [3]).

4. Discussion

ETCs are recognized as extreme atmospheric events. They are also known as winter storms, gales, and other tempests when they reach extreme intensities. They are, in fact, the main causes of weather-related disruptions and destructions over areas the size of a state or a country at mid- and high latitudes particularly along eastern oceanic seaboards such as the North Atlantic Eastern seaboard of the U.S and Canada. These result primarily from extreme winds but slow and extended floods, due to heavy precipitation, rain, snow, hail and grapple, are another hindrance, often leading to massive coastal erosion. Because of their large impact on navigation and circulation in general, ETCs have long been the focus of weather forecast and weather understanding. For some time when the first attempts of applying scientific reasoning to weather were undertaken, ETCs and TCs have been combined into the number one marine and coastal weather forecast problem. However, although their name somehow maintains this confusion within the language, they are quite distinct phenomena. One characteristic they do share, however, seen from the surface, is that the most intense ones seem to happen quite suddenly as a bad surprise. Predicting the occurrence of a mid-latitude storm with enough lead time has challenged forecasters for decades if not centuries. About every forecasting technique that has been devised ever since weather forecast is attempted has been applied to storm alert and has failed. It is only very recently that the best global prediction systems seem to have predicted most major events. One ambition of this article is to try to keep a link with real world ETCs as seen in real data.

To that end, we have documented the ocean atmospheric interaction during the formation and passage of an ETC storm, which occurred in the Cape Hatteras, southern apex of the Middle Atlantic Bight during the period 15-19 February 1996. Data collected (during the ambitious DOE Ocean Margins Program), from an Eulerian array of oceanographic and atmospheric moorings was used to create the sides of a CV. The data reveals details of the fueling of an atmospheric

low pressure system and also the interactive coupling between the atmospheric event and the ocean. The storm was shown to have extracted energy from the ocean in the form of latent and sensible heat. While coastal low pressure storms have been well documented ([2] [4]-[10]), more synoptic and comprehensive ocean and atmosphere observations of the interactive coupling have been lacking during the formation and passage of such an event.

During the progression of the storm, the heat entering the control volume through the sides was 4.62e+19 J while the heat exiting through the sides was −4.28e+19 J. This means there was a net increase of heat of 0.34e+19 J. The heat balance trough the surface of the CV as a result of sensible and latent heat fluxes and radiation was a net loss of −2.06e+18 J. Based on the area of the control volume, this value translates to an average surface heat flux of −596 W/m^2 during the event. The heat lost through the surface subtracted from the heat gained through the sides still shows an increase of 2.74e+18 J in the CV. This is a remarkable finding. The volumetric flux through the sides of the CV during the storm presence show more water entering than exiting which accounts for the observed 51 cm rise of water level along the coast. In addition, there was an estimated net increase in total volume and salt content in the CV over the storm event. The chain of events indicated by our analysis is that the storm was infused with energy from below as it passed over the CV, the subsequent storm wind-field then drove cold water from the MAB into the SAB and also relatively warm, saline waters from the Gulf Stream onto the continental shelf and into the CV.

5. Conclusion

ETCs are prominent winter storm features in the SAB and MAB region centered in the vicinity of Cape Hatteras North Carolina USA (Cione *et al.*, 1993). A field campaign happened to be underway in the region when, over the period 15-19 February 1996, an ETC was spawned and intensified near and within the region. This was a serendipitous event. The field campaign consisted of a heavily instrumented array of Eulerian atmospheric-oceanic moorings and the sensors were able to observe and document the interactively coupled atmospheric-oceanic processes during ETC genesis. In addition, a numerical model of the storm was employed and used to estimate the total heat fluxes from the ocean to atmosphere that fueled the storm. The observations reveal a climatological flywheel in this region of the planet that affects the movement of planetary heat from south to north. This is a topic for future studies.

Author Contributions

Pietrafesa was co-conceiver of the conceptualization of the study, designed the OMP observational field array, participated in the field program as the North Carolina State University (NCSU) PI, co-curated the data and was a principal contributor to the formal analysis and original writing of the manuscript. Churchill ran the ETA model, participated in the OMP field program as the Woods

Hole Oceanographic Institute PI, co-curated the data and was a contributor to the formal analysis and writing of the manuscript. Jacobs conducted his NCSU MS thesis using the data sets collected during the field program and was the principal in the original writing. Bao oversaw the methodology employed, provided software and did editing of the manuscript. Gayes provided the resources necessary for the conduct of the research and assisted in the editing of the manuscript.

Funding

This study was originally supported by the National Atmospheric and Oceanic Administration under Grant No. NA16RP2543 through the NOAA National Ocean Service's Charleston Coastal Service Center. Support for the data collection was provided by the U.S. Department of Energy under Grant No. DE-FG05-95ER62053. Support for the prior, basic processing of the data was provided by the National Science Foundation under Grant # OCE-98-18804. Dr. George Saunders of DOE is acknowledged for having conceived of the OMP. His foresight and dedication were foundational for the DOE OMP program which may have been the greatest ocean margins field program ever conducted in USA continental margin waters.

Data Availability Statement

The data used in this study are available from the U.S. Department of Energy Brookhaven National Laboratory and are available upon request at no cost for reproduction.

Conflicts of Interest

The authors declare no conflict of interest. The funders had no role in the design of the study; in the collection, analyses, or interpretation of data; in the writing of the manuscript, or in the decision to publish the results.

References

[1] Cione, J.J., Raman, S. and Pietrafesa, L.J. (1993) The Effect of Gulf Stream-Induced Baroclinicity on the U.S. East Coast Winter Cyclones. *Monthly Weather Review*, **121**, 421-430. https://doi.org/10.1175/1520-0493(1993)121<0421:TEOGSI>2.0.CO;2

[2] Bosart, L.F., Vaudo, C.J. and Helsdon Jr., J.H. (1972) Coastal Frontgenesis. *Journal of Applied Meteorology and Climatology*, **11**, 1236-1258. https://doi.org/10.1175/1520-0450(1972)011<1236:CF>2.0.CO;2

[3] Wang, X.L., Feng, Y., Compo, G.P., Swail, V.R., Zwiers, F.W., Allan, R.J., Sardeshmukh, P.D. (2013) Trends and Low Frequency Variability of Extra-Tropical Cyclone Activity in the Ensemble of Twentieth Century Reanalysis. *Climate Dynamics*, **40**, 2775-2800. https://doi.org/10.1007/s00382-012-1450-9

[4] Bosart, L.F. (1981) The Presidents' Day Snowstorm of 18-19 February 1979: A Synoptic-Scale Event. *Monthly Weather Review*, **109**, 1542-1566. https://doi.org/10.1175/1520-0493(1981)109<1542:TPDSOF>2.0.CO;2

[5] Rogers, E. and Bosart, L.F. (1986) An Investigation of Explosively Deepening Ocea-

nic Cyclones. *Monthly Weather Review*, **114**, 702-718.
https://doi.org/10.1175/1520-0493(1986)114<0702:AIOEDO>2.0.CO;2

[6] Holt, T. and Raman, S. (1990) Marine Boundary-Layer Structure and Circulation in the Region of Offshore Redevelopment of a Cyclone during GALE. *Monthly Weather Review*, **118**, 392-410.
https://doi.org/10.1175/1520-0493(1990)118<0392:MBLSAC>2.0.CO;2

[7] Davis, C.A. and Emanuel, K.A. (1988) Observational Evidence for the Influence of Surface Heat Fluxes on Rapid Maritime Cyclogenesis. *Monthly Weather Review*, **116**, 2649-2659. https://doi.org/10.1175/1520-0493(1988)116<2649:OEFTIO>2.0.CO;2

[8] Cione, J. and Pietrafes, L.J. (1998) The Use of Pre-Storm Boundary-Layer Baroclinicity in Determining and Operationally Implementing the Atlantic Surface Cyclone Intensification Index. *Boundary-Layer Meteorology*, **89**, 211-224.
https://doi.org/10.1023/A:1001773019199

[9] Xie, L., Pietrafesa, L.J. and Raman, S. (1999) Coastal Ocean-Atmosphere Coupling. *Coastal and Estuarine Studies*, **56**, 101-123.

[10] Sanders, F.J. and Gyakum, J.R. (1980) Synoptic-Dynamic Climatology of the "Bomb". *Monthly Weather Review*, **108**, 1589-1606.
https://doi.org/10.1175/1520-0493(1980)108<1589:SDCOT>2.0.CO;2

[11] Cione, J.J. and Raman, S. (1995) A Numerical Investigation of Surface-Induced Mesocyclogenesis Near the Gulf Stream. *Tellus*, **47A**, 815-833.
https://doi.org/10.1034/j.1600-0870.1995.00122.x

[12] Pietrafesa, L.J., Janowitz, G.S. and Whittman, J. (1985) Physical Oceanographic Processes in the Carolina Capes. *Coastal and Estuarine Science*, **2**, 23-33.

[13] Pietrafesa, L.J. and Janowitz, G.S. (1978) The Effects of Buoyancy Flux on Continental Shelf Circulation. *Journal of Physical Oceanography*, **10**, 1256-1263.

[14] Pietrafesa, L.J. and Janowitz, G.S. (1980) Gulf Stream Frontal Waves and Meanders. *Proceedings of the Trondheim Norway Conference on Oceanic Processes*, Vol. 1, Trondheim, June 1980, 51-69.

[15] Pietrafesa, L.J. (1975) Evidence for the Deflection of the Gulf Stream by the Charleston Rise. *Gulfstream*, **4**, 3-7

[16] Sun, L.C. and Pietrafesa, L.J. (1992) Baroclinic-Barotropic Instabilities and Energy Transfers in the Gulf Stream. In: Lakshmikantham, V., Ed., *World Congress of Nonlinear Analysts* '92: *Proceedings of the First World Congress of Nonlinear Analysts*, De Gruyter, Berlin, 3515-3532. https://doi.org/10.1515/9783110883237.3515

[17] Liu, W.T., Katsaros, K.B. and Businger, J.A. (1979) Bulk Parameterization of Air-Sea Exchanges of Heat and Water Vapor Including the Molecular Constraints at the Interface. *Journal of the Atmospheric Sciences*, **36**, 1722-1735.
https://doi.org/10.1175/1520-0469(1979)036<1722:BPOASE>2.0.CO;2

[18] Grossman, R.L. (1988) Boundary Layer Warming by Condensation: Air-Sea Interaction during an Extreme Cold Air Outbreak from the Eastern Coast of the United States. 7*th Conference on Oceanic-Atmospheric Interaction*, Anaheim, 31 January - 5 February 1988.

[19] Forbes, G.S., Thomson, D.W. and Anthes, R.A. (1987) Synoptic and Mesoscale Aspects of an Appalachian Ice Storm Associated with Cold-Air Damming. *Monthly Weather Review*, **115**, 564-591.
https://doi.org/10.1175/1520-0493(1987)115<0564:SAMAOA>2.0.CO;2

[20] Nowlin Jr., W.D. and Parker, C.A. (1974) Effects of a Cold-Air Outbreak on Shelf Waters of the Gulf of Mexico. *Journal of Physical Oceanography*, **4**, 467-486.

https://doi.org/10.1175/1520-0485(1974)004<0467:EOACAO>2.0.CO;2

[21] Lenschow, D.H., Wyngaard, J.C. and Pennel, W.T. (1980) Mean and Second-Moment Budgets in a Baroclinic Convective Boundary Layer. *Journal of the Atmospheric Sciences*, **37**, 1313-1326.

[22] Lenschow, D.H. and Agee, E.M. (1976) Preliminary Results from the Air Mass Transformation Experiment (AMTEX). *Bulletin of the American Meteorological Society*, **57**, 1346-1355. https://doi.org/10.1175/1520-0477-57.11.1346

[23] Chou, S.-H. and Atlas, D. (1982) Satellites Estimates of Ocean-Air Heat Fluxes during Cold-Air Outbreaks. *Monthly Weather Review*, **110**, 1434-1450. https://doi.org/10.1175/1520-0493(1982)110<1434:SEOOHF>2.0.CO;2

[24] Huh, O.K., Rouse Jr., L.J. and Walker, N.D. (1984) Cold Air Outbreaks over the Northwest Florida Contential Shelf: Heat Flux Processes and Hydrographic Changes. *Journal of Geophysical Research*: *Oceans*, **89**, 717-726. https://doi.org/10.1029/JC089iC01p00717

[25] Chou, S.-H., Atlas, D. and Yeh, E.-N. (1986) Turbulence in a Convective Marine Atmospheric Boundary Layer. *Journal of the Atmospheric Sciences*, **43**, 547-564. https://doi.org/10.1175/1520-0469(1986)043<0547:TIACMA>2.0.CO;2

[26] Raman, S., Riordan, A.J., Holt, T., Stunder, M. and Hinman, J. (1986) Observations of the Marine Boundary Layer Thermal Structure over the Gulf Stream during a Cold Air Outbreak. *Journal of Applied Meteorology and Climatology*, **25**, 14-21. https://doi.org/10.1175/1520-0450(1986)025<0014:OOTMBL>2.0.CO;2

[27] Wayland, R. and Raman, S. (1989) Mean and Turbulent Structure of a Baroclinic Marine Boundary Layer during the 28 January 1986 Cold-Air Outbreak (GALE 86). *Boundary-Layer Meteorology*, **48**, 227-254. https://doi.org/10.1007/BF00158326

[28] Reddy, N.C. and Raman, S. (1994) Scales and Spectra of Turbulence over the Gulf Stream. *Boundary-Layer Meteorology*, **68**, 387-417. https://doi.org/10.1007/BF00706798

[29] Li, X., Pietrafesa, L.J., Xie, L., Shaw, P.T. and Cione, J.J. (1997) The Climatology of Northwestern Atlantic Extratropical Cyclone Tracks over the Period 1983-1993. *Monthly Weather Review*, **125**, 1312-1341.

[30] Pietrafesa, L.J., Flagg, C.N., Xie, L., Weatherly, G.L. and Morrison, J.M. (2002). The Winter/Spring 1996 OMP Current, Meteorological, Sea State and Coastal Sea Level Fields. *Deep Sea Research Part II*: *Topical Studies in Oceanography*, **49**, 4331-4354. https://doi.org/10.1016/S0967-0645(02)00166-2

[31] Janjić, Z.I. (1994) The Step-Mountain Eta Coordinate Model: Further Developments of the Convection, Viscous Sublayer, and Turbulence Closure Schemes. *Monthly Weather Review*, **122**, 927-945. https://doi.org/10.1175/1520-0493(1994)122<0927:TSMECM>2.0.CO;2

[32] Black, T.L. (1994) The New NMC Mesoscale Eta Model: Description and Forecast Examples. *Weather and Forecasting*, **9**, 265-278. https://doi.org/10.1175/1520-0434(1994)009<0265:TNNMEM>2.0.CO;2

[33] Rogers, E., Black, T.L., Deaven, D. G., DiMego, G. J., Zhao, Q., Baldwin, M. and Junker, N. and Lin, Y. (1996) Changes to the Operational "Early" Eta Analysis/Forecast System at the National Centers for Environmental Prediction. *Weather and Forecasting*, **11**, 391-413. https://doi.org/10.1175/1520-0434(1996)011<0391:CTTOEA>2.0.CO;2

[34] Caplan, P., Derber, J., Gemmill, W., Hong, S.-Y., Pan, H.-L. and Parrish, D. (1997) Changes to the 1995 NCEP Operational Medium-Range Forecast Model Analysis-Forecast System. *Weather and Forecasting*, **12**, 581-594.

https://doi.org/10.1175/1520-0434(1997)012<0581:CTTNOM>2.0.CO;2

[35] Mesinger, F., Janjić, Z.I., Ničković, S., Gavrilov, D. and Deaven, D.G. (1988) The Step-Mountain Coordinate: Model Description and Performance for Cases of Alpine Lee Cyclogenesis and for a Case of an Appalachian Redevelopment. *Monthly Weather Review*, **116**, 1493-1517. https://doi.org/10.1175/1520-0493(1988)116<1493:TSMCMD>2.0.CO;2

[36] Pietrafesa, L.J., Epps, J., Weatherly, G. and Flagg, C. (1997) Ocean Margins Program Current, Meteorological, Wave and Sea Level Fields: February-May and June-October, 1996. NCSU/MEAS Technical Report No. 2001-6. NC State University, Raleigh, 222 p.

[37] McClain, E.P., Pichel, W.G. and Walton, C.C. (1985) Comparative Performance of AVHRR-Based Multichannel Sea Surface Temperatures. *Journal of Geophysical Research*: *Oceans*, **90**, 11587-11601. https://doi.org/10.1029/JC090iC06p11587

[38] Janowitz, G.S. and Pietrafesa, L.J. (1979) Time Dependent Upwelling on a Continental Shelf: Model and Observations. *Journal of Physical Oceanography*, **10**, 1574-1583.

[39] Janowitz, G.S. and Pietrafesa, L.J. (1996) Subtidal Frequency Fluctuations in Coastal Sea Level in the Mid and South Atlantic Bights: A Prognostic for Coastal Flooding. *Journal of Coastal Research*, **12**, 79-89.

[40] Pietrafesa, L.J., Morrison, J.M., McCann, M.P., Churchill, J., Böhm, E. and Houghton, R.W. (1994) Water Mass Linkages between the Middle and South Atlantic Bights. *Deep Sea Research Part II*: *Topical Studies in Oceanography*, **41**, 365-389. https://doi.org/10.1016/0967-0645(94)90028-0